A continuum theory for erosion in granular media

Ioannis Vardoulakis,* Euripides Papamichos**

Summary

A continuum theory for erosion in relation to the sand production problem in reservoir sandstones is presented. The theory regards the continuum as a three-phase medium and establishes a set of mass balance equations for the various phases. The solution of the problem requires an additional equation in the form of a constitutive or evolution law. Two laws are proposed in order to reproduce experimental evidence of a decreasing over time sand production rate.

1. Introduction

Sand production often occurs in the petroleum industry as the result of erosion in reservoir sandstones during hydrocarbon production. In such as a case, the rock around a wellbore or perforation is plastified, decohesioned and weakened as the result of the stress concentrations around the cavity due to the in situ stresses. The weakened and decohesioned rock may then be eroded away by the produced fluid. The prediction of the amount of produced sand and how it is affected by the applied stresses and flow rates over time are important for safe and economical hydrocarbon production. In the past, a continuum theory of erosion for sand production was formulated and applied to radial flow by VARDOULAKIS *et al.* [1995] and to axial flow by VARDOULAKIS *et al.* [2001]. Fluid flow erosion was coupled with the poro-mechanical behavior of a cavity under compression by STAVROPOULOU *et al.* [1998] and PAPAMICHOS and STAVROPOULOU [1998]. WAN and WANG [2000] provided numerical solutions for erosion without the influence of the stress field. Various ways of coupling fluid flow erosion and poro-mechanical behavior were proposed by PAPAMICHOS *et al.* [2001] on the basis of volumetric sand production experimental data on a sandstone.

The theory of erosion contains a constitutive law related to the rate of mass produced and various such laws may be introduced according to the physical mechanisms of sand production in order to describe experimental results. The constitutive law that has been employed so far results in a mass production rate constant over time. However, recent preliminary results in a variety of sandstones indicate that the mass production rate decreases over time. In this paper, two alternative constitutive laws are introduced to describe the observation of a reduced mass rate over time. The first law is inspired from filtration theories in the form of an evolution law for the particle concentration in the fluid. The second law suggests that the eroded particle discharge follows a gradient law that enforces particles to exit from regions of increasing porosity and result in a porosity diffusion equation, which is solved with the appropriate boundary conditions.

* Faculty of Applied Sciences, Department of Mechanics, National Technical University of Athens, Greece.

** Dept. of Civil Engineering, Aristotle University of Thessaloniki, Greece.

2. Formulation

2.1. Three-phase medium

The porous rock is viewed as a three-phase medium with a representative volume element dV, shown in Fig. 1, consisting of (1) solid grains (s) with volume dV_s, (2) fluid (f) with volume dV_f, and (3) fluidized grains (fs) with volume dV_{fs}. The void space dV_v is fully fluid-saturated and thus $dV_v = dV_f$. The porosity ϕ and the concentration c of fluidized solids in the fluid are defined as

$$\phi = \frac{dV_v}{dV} = \frac{dV_f}{dV} \qquad c = \frac{dV_{fs}}{dV_f} \tag{1}$$

The partial densities for the three phases are defined as

$$\rho^{(1)} = \frac{dm_s}{dV} = \rho_s \frac{dV_s}{dV} = \rho_s \frac{dV - (dV_f + dV_{fs})}{dV} = \left[1 - (1+c)\phi\right]\rho_s \tag{2}$$

$$\rho^{(2)} = \frac{dm_f}{dV} = \rho_f \frac{dV_f}{dV} = \rho_f \frac{\phi dV}{dV} = \phi \rho_f \tag{3}$$

$$\rho^{(3)} = \frac{dm_{fs}}{dV} = \rho_s \frac{dV_{fs}}{dV} = \rho_s \frac{c\phi dV}{dV} = c\phi\rho_s \tag{4}$$

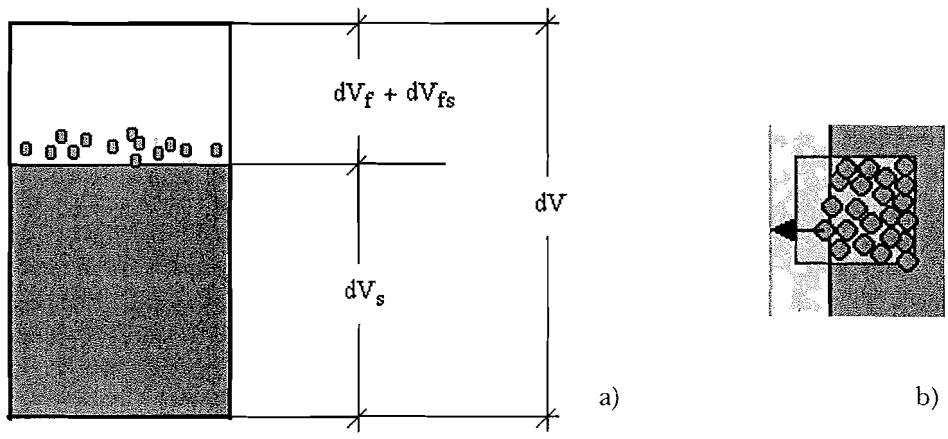

Fig. 1 - (a) Three-phase medium diagram and (b) Partially detached fluidized particles.
Fig. 1 – (a) Schema del materiale trifase (b) Particelle parzialmente fluidizzate.

where ρ_s is the density of the solid constituents and ρ_f the fluid density. Definition Eq. (2) differs from the one presented earlier [VARDOULAKIS *et al.*, 1995] and results in some simplifications in the formulation. The total density ρ of the mixture is

$$\rho = \frac{dm}{dV} = \frac{dm_s + dm_f + dm_{fs}}{dV} = \rho^{(1)} + \rho^{(2)} + \rho^{(3)} = \\ = (1-\phi)\rho_s + \phi\rho_f \tag{5}$$

The velocities of the three phases are $v_i^{(1)}$, $v_i^{(2)}$, $v_i^{(3)}$. It is assumed that the solid skeleton is rigid and that the velocity of the fluidized particles is equal to the fluid velocity, i.e.

$$v_i^{(1)} = 0 \\ v_i^{(3)} = v_i^{(2)} \tag{6}$$

In general the velocity of the fluidized particles is a fraction of the fluid velocity, say $v_i^{(3)} = \xi v_i^{(2)}$ with $0 < \xi \leq 1$. Experimental results on filtration processes suggest that $\xi \approx 0.5$ [ADEL and BAKKER, 1993]. In such a case, instead of Eq. (6)b it may be assumed that the velocity of the fluidized grains is the mean value of the velocity of the grains and the velocity of the fluid, i.e. $v_i^{(3)} \approx (v_i^{(1)} + v_i^{(2)})/2 = v_{i/2}^{(2)}$. The volume discharges for the fluid and the fluidized solids are related to the velocity as follows [cf. VARDOULAKIS and SULEM, 1995]

$$q_i^{(2)} = \frac{dV_f}{dS_i dt},\quad v_i^{(2)} = \frac{dV_f}{dS_i^{(2)} dt},\quad dS_i^{(2)} \approx \phi dS_i \Rightarrow q_i^{(2)} = \phi v_i^{(2)}$$

$$q_i^{(3)} = \frac{dV_{fs}}{dS_i dt},\quad v_i^{(3)} = v_i^{(2)},\quad dS_i^{(3)} \approx c\phi dS_i \Rightarrow q_i^{(3)} = c\phi v_i^{(2)} = c q_i^{(2)} \tag{7}$$

Thus the total discharge is

$$\bar{q}_i = q_i^{(2)} + q_i^{(3)} = (1 + c)\phi v_i^{(2)} \tag{8}$$

By using the definition of the relative specific discharge for the fluid

$$q_i = \phi(v_i^{(2)} - v_i^{(1)}) = \phi v_i^{(2)} = q_i^{(2)} \tag{9}$$

the total discharge becomes

$$\bar{q}_i = (1 + c) q_i \tag{10}$$

2.2. Mass balance

Mass balance for the solid phase is expressed on the basis of the definitions for the partial densities and the velocities of the species as

$$\frac{\partial \rho^{(1)}}{\partial t} + div(\rho^{(1)} v_i^{(1)}) = j^{(1)} \tag{11}$$

The term $j^{(1)}$ on the right-hand side of this equation represents the rate of produced mass (here removed due to erosion). With Eqs. (2) and (6), it becomes

$$\frac{\partial}{\partial t}[(1+c)\phi] = -\frac{j^{(1)}}{\rho_s} \tag{12}$$

Similarly, mass balance for the fluidized solid phase is expressed as

$$\frac{\partial \rho^{(3)}}{\partial t} + div(\rho^{(3)} v_i^{(3)}) = j^{(3)} \tag{13}$$

Using Eqs. (4) and (6) and the definition Eq. (9) for the relative specific discharge for the fluid, yields

$$\frac{j^{(3)}}{\rho_s} = \frac{\partial (c\phi)}{\partial t} + div(\alpha\phi v_i^{(3)}) = \frac{\partial (c\phi)}{\partial t} + div(c q_i^{(3)}) = \\ = \frac{\partial (c\phi)}{\partial t} + div q_i \tag{14}$$

Taking into account that all eroded mass stems from the solid skeleton, i.e.

$$j^{(3)} = -j^{(1)} \tag{15}$$

and eliminating the mass generation term using Eq. (12) results in a mass balance equation, which relates the changes in porosity to the flux of fluidized particles $q_i^{(3)}$

$$\frac{\partial \phi}{\partial t} = div(cq_i) = divq_i^{(3)} \tag{16}$$

Finally, mass balance for the fluid phase is written as

$$\frac{\partial \rho^{(2)}}{\partial t} + div\left(\rho^{(2)} v_i^{(2)}\right) = 0 \tag{17}$$

and through Eqs. (3) and (9) yields

$$\frac{\partial \phi}{\partial t} + divq_i = 0 \tag{18}$$

Use of Eq. (16) yields a continuity equation for the total discharge $\bar{q}_i$

$$div\bar{q}_i = 0 \tag{19}$$

The fluid flow flux q_i can be expressed through the pore pressure p using Darcy's law

$$q_i = -\frac{k}{\eta}\frac{\partial p}{\partial x_i} \tag{20}$$

where k is the physical rock permeability and η the fluid viscosity. The permeability k is in general a function of the porosity. For example the Carman-Kozeny law suggests that [cf. BEAR, 1972]

$$k = k_c \frac{\phi^3}{(1-\phi)^2} \tag{21}$$

where k_c is a permeability parameter independent of the porosity of the rock. Thus in a process where the porosity changes locally in time due to erosion, fluid-flow in the pore space becomes a non-linear phenomenon controlled by the particle erosion.

Eqs. (12), (16) and (19) constitute a set of three mass balance equations for the considered three-phase medium, which hold under the assumption Eq. (6) for the partial velocities. This set of equations contains four independent unknown quantities, the porosity ϕ, the concentration c, the rate of produced mass $j^{(1)}$, and the pore fluid pressure p. Thus one additional equation is required for the solution of the erosion problem. This equation is provided in the form of an evolution or constitutive law for erosion. Various constitutive laws can be proposed depending on the physics of problem. Previously, a form where erosion is driven by the fluid flux was proposed for the sand production problem [PAPAMICHOS *et al.*, 2001] or a form where erosion is driven by the discharge of fluidized particles [PAPAMICHOS and STAVROPOULOU, 1998; VARDOULAKIS *et al.*, 1996; STAVROPOULOU *et al.*, 1998]. In the following two different constitutive model laws are put forward.

2.3. *Filtration model*

The first model is inspired by the one-dimensional filtration theory where mass is absorbed by the solid matrix and which states that the concentration gradient is proportional to the concentration, i.e. $\partial c/\partial x = -\Lambda c$, where $\Lambda > 0$ is an experimentally determined parameter with dimension of inverse length [IWASAKI, 1937]. Iwasaki's theory may be extended to a power law of the form $\partial c/\partial x = -\Lambda c^n$, which in the present context suggests the following evolution law for the fluidized particle concentration c

$$\dot{c} = -\Lambda c^n \, \| q_i \| \tag{22}$$

where $\| \cdot \|$ denotes the norm of a vector and $\dot{c}$ is the material time derivative of c, i.e.

$$\dot{c} = \frac{D^{(3)}c}{Dt} = \frac{\partial c}{\partial t} + v_i^{(3)}\frac{\partial c}{\partial x_i} \tag{23}$$

or

$$\phi\dot{c} = \phi\frac{\partial c}{\partial t} + q_i\frac{\partial c}{\partial x_i} \quad \Rightarrow \quad \phi\frac{\partial c}{\partial t} = \phi\dot{c} - q_i\frac{\partial c}{\partial x_i} \tag{24}$$

Using Eq. (24) the mass generation term $j^{(1)}$ in Eq. (12) is evaluated as

$$-\frac{j^{(1)}}{\rho_s} = (1+c)\frac{\partial \phi}{\partial t} + \phi\dot{c} - q_i\frac{\partial c}{\partial x_i} \tag{25}$$

which with the help of Eqs. (18) and (10) yields

$$\begin{aligned} -\frac{j^{(1)}}{\rho_s} &= \phi\dot{c} - (1+c)\frac{\partial q_i}{\partial x_i} - q_i\frac{\partial c}{\partial x_i} = \\ &= \phi\dot{c} - \frac{\partial}{\partial x_i}\left[(1+c)q_i\right] = \phi\dot{c} - div\bar{q}_i \end{aligned} \tag{26}$$

Using Eqs. (15) and (19), Eq. (26) yields that the mass generation term $j^{(3)}$, i.e. the mass added to the fluid due to erosion of the skeleton, is given by the

material time derivative with respect to the fluid phase of the fluidized particle concentration

$$\frac{j^{(3)}}{\rho_s} = \phi \dot{c} \tag{27}$$

This can be combined with the constitutive law for erosion Eq. (22) to obtain

$$\frac{j^{(3)}}{\rho_s} = \Lambda \phi c^n \|q_i\| \tag{28}$$

2.4. Porosity diffusion model

The second constitutive model describes erosion in mono-disperse media as opposed to filtration of fines in a coarse matrix. In this case it does not exist yet a well-established evolution model and various propositions can be made. All theories are based on a limited experimental database that is presently developed in various specialized laboratories.

The governing mass balance Eq. (16) for the eroded particle discharge velocity $q_i^{(3)}$ states that all porosity changes in a volume of rock is due to the net transport of grains outside this volume, as shown in Fig. 2. A simple model for the eroded particle discharge is a gradient law that enforces particles to exit from regions of increasing porosity, as shown in Fig. 3. This can be written as

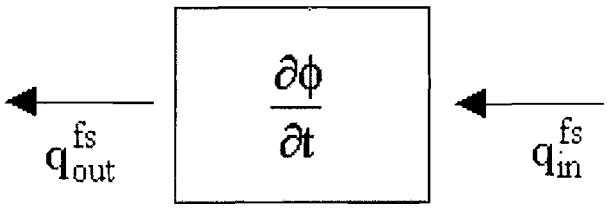

Fig. 2 – On the transport equation.
Fig. 2 – Rappresentazione equazione del trasporto.

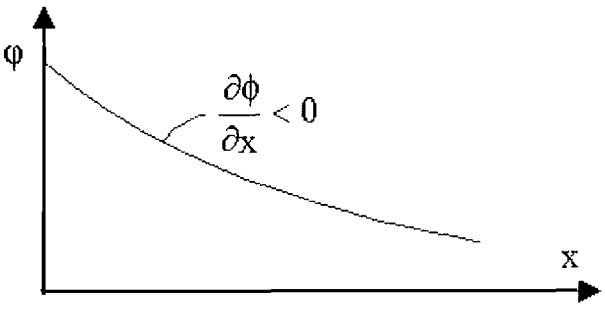

Fig. 3 – The least resistance law for particle erosion.
Fig. 3 – Legge di minimia resistenza per l'erosione delle particelle.

$$q_i^{(3)} = \lambda \frac{\partial \phi}{\partial x_i} \tag{29}$$

and can be viewed as a 'piping' erosion law which enforces the flow lines of the eroded particles to follow the porosity gradient. Combination of Eqs. (16) and (29) results in a porosity diffusion law

$$\frac{\partial \phi}{\partial t} = \frac{\partial}{\partial x_i}\left(\lambda \frac{\partial \phi}{\partial x_i}\right) \tag{30}$$

The parameter λ with dimensions length squared over time plays the role of a porosity diffusivity coefficient. If λ is assumed constant, the above porosity diffusion equation becomes a heat conduction-type equation

$$\frac{\partial \phi}{\partial t} = \lambda \frac{\partial^2 \phi}{\partial x_i^2} \tag{31}$$

This model has the advantage of uncoupling the porosity from the coupled set of equations and thus solve the problem analytically for certain geometries and/or boundary and initial conditions. In the following the porosity diffusion model is applied to the cavity test.

3. The cavity test

The typical test for studying erosion in petroleum engineering is the so-called cavity test. An example of a cavity test setup is the volumetric sand production experiment at SINTEF Petroleum Research where a thick-wall hollow cylinder of oil-saturated rock is placed under confining stress with oil flown radially from the external surface towards the inner cavity. Fig. 4 shows a schematic of a horizontal section of the specimen and the applied boundary conditions. The test is defined by the following test parameters: (i) Internal cavity radius R_i, (ii) External specimen radius R_e, (iii) Specimen height H, (iv) External confining pressure σ_c, (v) Zero pore-fluid pressure in the cavity $p_i = 0$, and (vi) External pore-fluid pressure p_e. During the test the following discharges are monitored over time: (i) Total oil flow Q_f in [m^3/s], and (ii) Cumulative produced sand mass M_s from the cavity in [kg]. From these quantities one can compute averages, namely the: (i) Specific fluid discharge at the cavity $q_R = Q_f / A$ [m/s], and (b) The cumulative sand mass produced per unit cavity area $m_s = M_s / A$ [kg/m^2] where $A = 2\pi R_i H$ the cavity surface area.

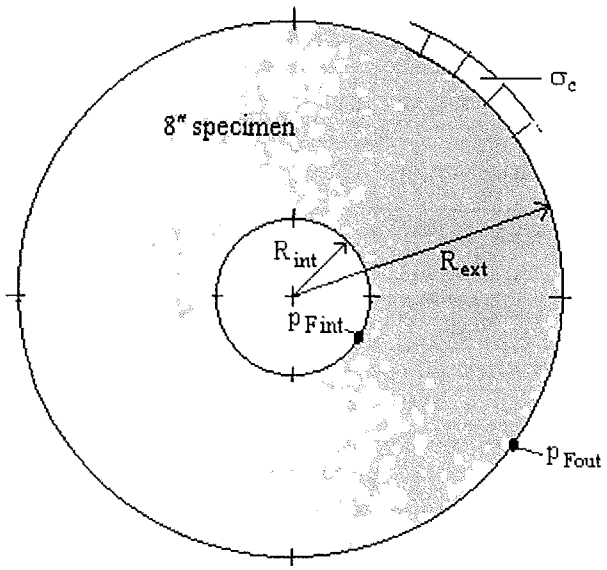

Fig. 4 - Schematic of a horizontal section of the specimen in the cavity test.
Fig. 4 – Sezione orizzontale del provino utilizzato nel "cavity test".

For axisymmetric radial flow conditions, the continuity Eq. (19) for the total fluid discharge is written as

$$\frac{\partial \bar{q}_r}{\partial r} + \frac{\bar{q}_r}{r} = 0 \tag{32}$$

with solution $\bar{q}_r(t) = -\bar{q}_R(t)R_i/r$. In the experiment, the concentration remains always small, i.e. $0 < c << 1$ and thus $\bar{q}_R(t) = (1 + c)\bar{q}_R \approx \bar{q}_R$. Darcy's law Eq. (20) may then be applied for the total discharge as

$$\bar{q}_r = -\frac{k}{\eta}\frac{\partial p}{\partial r} \tag{33}$$

and with the continuity Eq. (32) yields

$$\frac{\partial^2 p}{\partial r^2} + \left(\frac{1}{r} + \frac{1}{k}\frac{dk}{d\phi}\frac{\partial \phi}{\partial r}\right)\frac{\partial p}{\partial r} = 0 \tag{34}$$

where for the Carman-Kozeny permeability model

$$\frac{1}{k}\frac{dk}{d\phi} = \frac{3-\phi}{\phi(1-\phi)} \tag{35}$$

For axisymmetric radial flow the porosity diffusion constitutive Eq. (31) becomes

$$\frac{\partial \phi}{\partial t} = \lambda\left(\frac{\partial^2 \phi}{\partial r^2} + \frac{1}{r}\frac{\partial \phi}{\partial r}\right) \tag{36}$$

The appropriate initial and boundary conditions for the cavity test are needed to solve mathematically Eq. (36). During the test, the pore pressure at the cavity remains at zero and at the external surface of the specimen is kept constant, i.e.

$$\begin{aligned} p(R_i, t \geq 0) &= 0 \\ p(R_e, t \geq 0) &= p_e = const \end{aligned} \tag{37}$$

Initially the porosity in the specimen is constant and equal to ϕ_0, i.e.

$$\phi(r, t = 0) = \phi_0 = const, \qquad R_i \leq r \leq R_e \tag{38}$$

which results in a logarithmic radial profile for the initial pore pressure

$$p(r, t=0) = \frac{\eta R_i q_R(0)}{k(\phi_0)} \ln\frac{r}{R_i} \tag{39}$$

For the porosity it is assumed that the erosion process is confined within a ring-shaped damage zone close to the cavity, that is in the annulus $R_i \leq r \leq R_d << R_e$ where the rock is converted into sand due to stress-induced de-cohesioning (strain-softening). The porosity inside the external intact region $R_d \leq r \leq R_e$ is assumed to be constant and equal to its initial value. Thus the external boundary condition is

$$\phi(R_d, t \geq 0) = \phi_0 \tag{40}$$

To establish the necessary second boundary condition, it is assumed that the discharge of fluidized particles at the exit point is proportional to the total discharge

$$q_r^{(3)}(r = R_i, t > 0) = \alpha \bar{q}_r(r = R_i, t > 0) \tag{41}$$

This assumption together with Darcy's law Eq. (33) and the constitutive Eq. (29) for the fluidized-particles discharge yield the following Neumann-type, configuration-dependent boundary condition for the porosity

$$\left.\frac{\partial \phi}{\partial r}\right|_{r=R_i} = -C_\phi \frac{k(\phi)}{\eta}\left.\frac{\partial p}{\partial r}\right|_{r=R_i} \tag{42}$$

where $C_\phi = \alpha/\lambda$ is an open problem parameter with dimensions time over length squared and may be evaluated experimentally.

3.1. Mathematical formulation and numerical results

The initial boundary value problem at hand is governed by the partial differential Eqs. (34) and (36), the initial conditions (38) and (39) and the boundary conditions (37), (40) and (42). For the ma-

thematical treatment of the problem, the following non-dimensional variables are introduced

$$r^* = \frac{r}{R_i} \qquad t^* = \frac{\lambda}{R_i^2} t \qquad p^* = \frac{p}{p_e} \tag{43}$$

and the governing equations and the initial and boundary conditions become

Eq. (36): $$\frac{\partial \phi}{\partial t^*} = \frac{\partial^2 \phi}{\partial r^{*2}} + \frac{1}{r^*} \frac{\partial \phi}{\partial r^*} \tag{44}$$

Eq. (34): $$\frac{\partial^2 p^*}{\partial r^{*2}} + \left(\frac{1}{r^*} + \frac{1}{k} \frac{dk}{d\phi} \frac{\partial \phi}{\partial r^*} \right) \frac{\partial p^*}{\partial r^*} = 0 \tag{45}$$

(i.c.1): $$p^*(r^*, t = 0) = \frac{\ln r^*}{\ln R_e^*} \qquad 1 \le r^* \le R_e^* \tag{46}$$

(b.c.1): $$p^*(1, t^* > 0) = 0$$
$$p^*(R_e^*, t^* > 0) = 1 \tag{47}$$

(i.c.2): $$\phi(r^*, t^* = 0) = \phi_0 \qquad 1 \le r^* \le R_e^* \tag{48}$$

(b.c.2): $$\left. \frac{\partial \phi}{\partial r^*} \right|_{r^*=1} = -C_\phi \frac{k p_e}{\eta} \left. \frac{\partial p^*}{\partial r^*} \right|_{r^*=1} \tag{49}$$
$$\phi(R_d^*, t^* \ge 0) = \phi_0$$

From these equations the pore-fluid pressure and porosity distribution can be computed numerically by using for example a finite difference scheme. The volumetric sand produced at the cavity surface can be evaluated from the numerical solution for the porosity distribution and evolution. The mass discharge of eroded particles is

$$\dot{m}_s = -p_s q_r^{(3)} = -p_s c q_r \tag{50}$$

Eq. (16) in a cylindrical coordinate system gives

$$\frac{\partial \phi}{\partial t} = \frac{1}{r} \frac{\partial}{\partial r} (r c q_r) \tag{51}$$

and with that we obtain

$$\frac{1}{r} \frac{\partial}{\partial r} (r \dot{m}_s) = -\rho_s \frac{\partial \phi}{\partial t} \quad \Rightarrow \quad \dot{m}_s = -\frac{\rho_s}{r} \int_{R_i}^{R_d} \frac{\partial \phi}{\partial t} r dr \tag{52}$$

Thus at the cavity wall the sand rate per cavity area is

$$\dot{m}_s(r = R_i) = \frac{\rho_s}{R_i} \int_{R_i}^{R_d} \frac{\partial \phi}{\partial t} r dr \quad \Rightarrow$$

$$\Rightarrow \quad m_s(r = R_i, t) = \frac{\rho_s}{R_i} \int_{R_i}^{R_d} \phi(r, t) r dr - \frac{\rho_s (R_d^2 - R_i^2) \phi_0}{2 R_i} \tag{53}$$

Tab. I – Cavity test input parameters.
Tab. I – Parametri d'ingresso nella "cavity simulation".

Cavity radius R_i [m]	0.01	Permeability parameter k_c [m^2]	7.5E-13
External radius R_e [m]	0.1	Oil viscosity η_{oil} [MPa·s]	3.6E-9
Damage zone radius R_d [m]	0.02	Sand prod. coeff. λ [m^2/s]	1.E-7
External pore pressure p_e [MPa]	0.5	C_ϕ [s/m^2]	1.8E-6
Initial porosity ϕ_0 [-]	0.3		

or

$$m_s(r^* = 1, t^*) = \rho_s R_i \int_1^{R_d^*} \phi(r^*, t^*) r^* dr^* - \frac{\rho_s (R_d^2 - R_i^2) \phi_0}{2 R_i} \tag{54}$$

The total discharge at the cavity wall is given by Darcy's law as

$$\bar{q}_R(t) = \frac{k(\phi) p_e}{\eta R_i} \left. \frac{\partial p^*}{\partial r^*} \right|_{r^*=1} \tag{55}$$

Fig. 5 and Fig. 6 summarize the results of an evaluation of the above set of equations for the typical set of problem parameters listed in Tab. I. Fig. 5 shows the cumulative sand production with time. The sand production rate, i.e. the slope of the curve, decreases with time, which has been observed in tests in the laboratory and the field. Fig. 6 shows a radial profile of the porosity at an intermediate time.

4. Concluding remarks

A framework for the continuum-mechanical description of sand erosion processes was presented. The model is based on mass-balance considerations, on Darcy's law and on a constitutive law for the flow of fluidized sand particles. According to the constitutive Eq. (29) it was assumed that fluidized sand particles follow a path of least resistance, namely the pathway of the porosity gradient. This assumption is a continuum-mechanical interpretation of the so-called 'piping' phenomenon. In addition, it is necessary to introduce a condition at the boundary where particles exit the rock formation. We adopted here a law with Eq. (41) that relates the normal-to-the-boundary component of the fluidized-particles discharge vector to the total discharge. The model predicts a sand rate that decreases with time. This is in accordance with recent experimental results and field observations. Earlier models [PAPAMICHOS *et al.*, 2001] were develo-

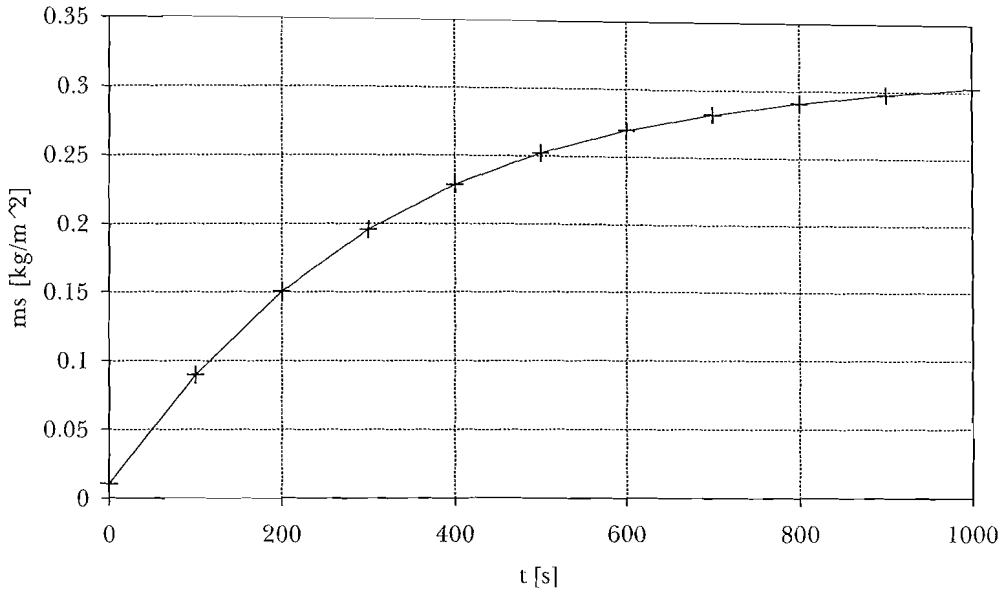

Fig. 5 – Sand production at the cavity wall as a function of time.
Fig. 5 – "Sand production" sulla parete della cavità in funzione del tempo.

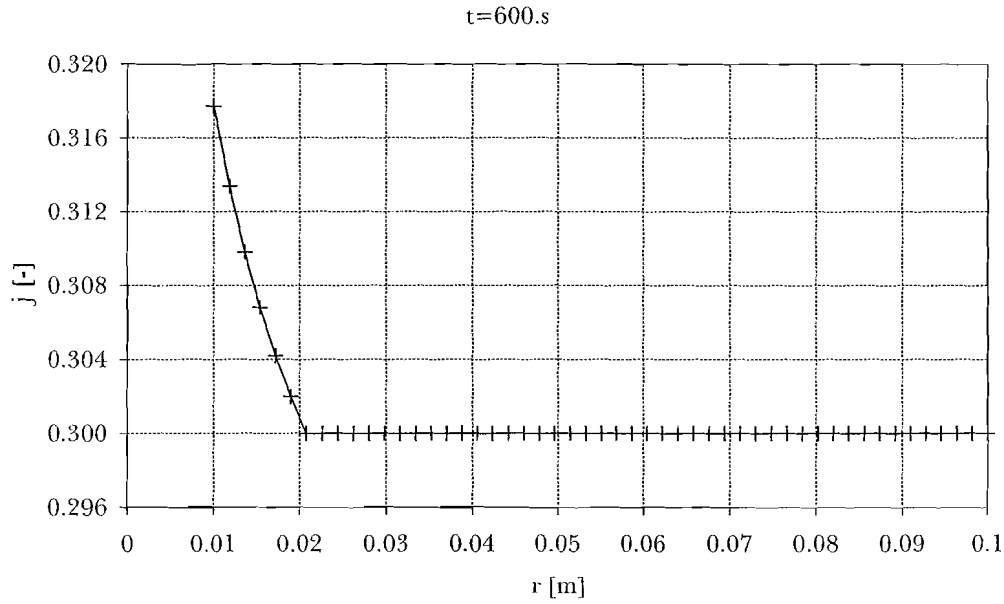

Fig. 6 – Radial porosity distribution at an intermediate time.
Fig. 6 – Distribuzione radiale della porosità in una fase intermedia.

ped to give a constant sand rate over time. The selection of the constitutive set of Eqs. (29) and (41) must thus be scrutinized with a broad experimental database. In a future publication the authors will provide such a critical discussion of this and other possible variants of the sand erosion model. The presented model treats only the hydraulic part of the sand production problem and does not consider the rock mechanical part, i.e. the applied stresses around the cavity that cause the rock to fail and become available for erosion. The mechanical part is only reflected in the decohesioned zone radius R_d. At low stresses compared to the rock strength, $R_d = R_i$ and no sand production is possible. Above a certain value for the stresses $R_d > R_i$ and sand production begins. R_d increases as the stresses increase and sand is produced. A coupled hydro-mechanical model that includes the effect of the stresses on the decohesioned zone has been presented and used for a comparison of predictions with test and field data [PAPAMICHOS *et al.*, 2001; PAPAMICHOS and MALMANGER, 2001].

Acknowledgments

The authors wish to thank the sponsors of the SINTEF Petroleum Research 'Volumetric Sand Production' project, Conoco Norway, Norsk Hydro, Shell International Exploration and Production and Statoil for supporting this research.

References

ADEL H. DEN, BAKKER K.J. (1993) – *A transport model for filtration: Control of erosion processes*. Filters in Geotechnical and Hydraulic Engineering, Brauns *et al.* (eds), Balkema.

BEAR J. (1972) – *Dynamics of Fluids in Porous Media*, Dover.

Iwasaki T. (1937) – *Some notes on sand filtration*. J. Amer. Water Works Assoc., 29, pp. 1591-1602.

PAPAMICHOS E., MALMANGER E.-M. (2001) – *A Sand Erosion Model for Volumetric Sand Predictions in a North Sea Reservoir*. SPE 54007, SPE Reservoir Evaluation & Engineering, February, pp. 44-50.

PAPAMICHOS E., STAVROPOULOU M. (1998) – *An erosion-mechanical model for sand production rate prediction*. Int. J. Rock Mech. Min. Sci., 35, pp. 531-532.

PAPAMICHOS E., VARDOULAKIS I., TRONVOLL J., SKJÆRSTEIN A. (2001) – *Volumetric sand production model and experiment*. Int. J. Numer. Anal. Methods Geomech., 25, pp. 789-808.

STAVROPOULOU M., PAPANASTASIOU P., VARDOULAKIS I. (1998) – *Coupled wellbore erosion and stability analysis*. Int. J. Numer. Anal. Methods Geomech., 22, pp. 749-769.

VARDOULAKIS I., PAPANASTASIOU P., STAVROPOULOU M. (2001) – *Sand erosion in axial flow conditions*. Transport in Porous Media, in print.

VARDOULAKIS I., STAVROPOULOU M., PAPANASTASIOU P. (1995) – *Hydromechanical aspects of sand production problem*. Transport in Porous Media, 22, pp. 225-244.

VARDOULAKIS I., SULEM J. (1995) – *Bifurcation Analysis in Geomechanics*. Blackie Academic and Professional.

WAN R.G., WANG J. (2002) – *Modelling sand production within a continuum mechanics framework*. Proc. Canadian Int. Conf. 2000, Calgary, Alberta, pp. 1-8.

Una teoria del continuo per l'erosione nei materiali granulari

Sommario

Si presenta una teoria per descrivere l'erosione che accompagna il fenomeno della "sand production" nei giacimenti in arenaria. Il materiale è trattato come un continuo composto da tre fasi, e la teoria poggia sulle equazioni di conservazione della massa. Al fine di risolvere il problema si introduce una ulteriore equazione che rappresenta l'evoluzione del fenomeno. In particolare vengono prese in considerazione due relazioni che sono in grado di riprodurre l'evidenza sperimentale secondo la quale la velocità di "sand production" diminuisce nel tempo.